

Discrete Adjoint-Based Simultaneous Analysis and Design Approach for Conceptual Aerodynamic Optimization

Oliviu SUGAR-GABOR*

*Corresponding author

Department of Aeronautical and Mechanical Engineering, School of Computing,
Science and Engineering, University of Salford,
The Crescent, M5 4WT, Salford, United Kingdom,
o.sugar-gabor@salford.ac.uk

DOI: 10.13111/2066-8201.2017.9.3.11

Received: 13 July 2017/ Accepted: 18 August 2017/ Published: September 2017

Copyright©2017. Published by INCAS. This is an “open access” article under the CC BY-NC-ND license (<http://creativecommons.org/licenses/by-nc-nd/4.0/>)

Abstract: *In this paper, a simultaneous analysis and design method is derived and applied for a non-linear constrained aerodynamic optimization problem. The method is based on the approach of defining a Lagrange functional based on the objective function and the aerodynamic model's equations, using two sets of multipliers. A fully-coupled, non-linear system of equations is derived by requiring that the Gateaux variation of the Lagrange functional vanishes for arbitrary variations of the aerodynamic model's dependent variables and design parameters. The optimization problem is approached using a one-shot technique, by solving the non-linear system in which all sensitivities and problem constraints are included. The computational efficiency of the method is compared against a gradient-based optimization algorithm using adjoint-provided gradient. A conceptual-stage aerodynamic optimization problem is solved, based on a non-linear numerical lifting-line method with viscous corrections.*

Key Words: *Simultaneous Analysis and Design, Adjoint-Based Optimization, Discrete Adjoint, Aerodynamic Optimization, Non-linear Lifting-Line Method*

1. INTRODUCTION

Aerodynamic optimization represents a discipline at the crossroads of several scientific and research areas such as geometry modelling, aerodynamic simulation, applied mathematics, non-linear optimization and computer science [1]. Because the use of high-fidelity CFD simulations in the aerodynamic design of aircraft has been steadily and rapidly increasing, the application of various optimization algorithms has been attempted, in an attempt to minimize the required number of CFD solutions and to increase the computational efficiency of the design and optimization process.

Jameson approached aerodynamic design and optimization procedures as control theory problems [2], and later popularized using the adjoint equation [3] for calculating the objective function gradient. The advantage of the adjoint method is that the computational effort required for evaluating the objective function gradient becomes independent of the number of design variables. In addition, the adjoint equations are of the same mathematical type as the equations governing the flow, and thus can be solved using the same numerical algorithms as for the flow equations.

Using the adjoint method, each design iteration requires one flow equations solution and one adjoint equations solution. This represents a very significant advantage over the finite-differences approach, where a number of flow equations solutions equal to the number of design variables is required to determine the objective function gradient. The optimization process and the values of the design variables are driven by a gradient-based constrained optimization algorithm, such as the Method of Feasible Directions (MFD), Sequential Quadratic Programming (SQP) or the penalty function augmented Broyden-Fletcher-Goldfarb-Shanno (BFGS) [4].

The implementation of the adjoint method in aerodynamic optimization using the Euler or Navier-Stokes equations has been carried out using two approaches: continuous adjoint and discrete adjoint [5]. In the first approach, the adjoint equations are deduced from the continuous form of the flow equations, and thus are also nonlinear partial-differential equations, requiring an appropriate set of boundary conditions. In the second approach, the adjoint equations are determined from the spatially and temporally-discretized flow equations, and thus will represent a linear system of equations, with any boundary conditions already included in the linear system terms.

Aerodynamic optimization using gradient-based optimization algorithms coupled with and adjoint-equation gradient computation have been extensively used over the last years, for a wide variety of problems across various industries. These include helicopter rotors [6], automobiles [7], wide-body transport aircraft [8] supersonic aircraft configurations [9], tidal turbines [10] and ship hulls [11].

Even with the increase in popularity of the adjoint approach, driven by the significant reduction in computational effort it provides, other algorithms such as non-deterministic global optimization algorithm are still commonly used in aerodynamic optimization problems, despite their relatively high computational costs. Similarly to the adjoint-method optimization, these algorithms have been applied to solve problems in a wide range of engineering applications. More recently, genetic algorithms (GA) have been used for wind turbine blades [12], for the shape optimization of a morphing wing wind tunnel technical demonstrator [13], [14], while the artificial bee colony (ABC) algorithm has been used for the numerical analysis of a UAV morphing wing [15]. A significant advantage of gradient-free global optimization algorithms is that they can be very easily configured to run on massively-parallel computers in order to reduce the overall execution time.

The present paper presents a methodology for further reducing the computational cost of the discrete adjoint method, with the construction of an adjoint-based simultaneous analysis and design technique. A Lagrange functional is defined based on the objective function and the aerodynamic model's equations, and by using two sets of Lagrange multipliers (which also represent the adjoint variables) [16], [17]. By imposing the requirement that the Gateaux variation of Lagrange functional vanish for arbitrary variations of the system dependent variables and design parameters, a set on non-linear equations is determined. The optimization problem of minimizing the objective function is then solved simultaneously with the aerodynamic model's equations, by using the one-shot approach, as the solution of the constructed non-linear system (which takes into consideration all sensitivities and imposed constraints).

2. MATHEMATICAL MODEL

When considering the discretized system of equations governing steady-state fluid flow around an aerofoil or wing, or the simplified aerodynamic models used throughout many

stages of aircraft conceptual design, the problem reduces to solving a system of algebraic equations. Let the algebraic system of linear or non-linear equations be:

$$\mathbf{R}(\mathbf{w}, \boldsymbol{\alpha}) = \mathbf{0}, \quad \mathbf{R}: \mathbb{R}^N \times \mathbb{R}^D \rightarrow \mathbb{R}^N \tag{1}$$

where $\mathbf{w} \in \mathbb{R}^N$ are the system dependent variables and $\boldsymbol{\alpha} \in \mathbb{R}^D$ are the system design parameters, whose values must be given in order to determine a solution for the system of equations.

The aerodynamic characteristics of aerofoil and wings, such as the lift and drag coefficients, the chord-wise pressure distribution or the span-wise lift distribution, are functions of both dependent variables and system parameters. The objective function to be minimised is given by:

$$J(\mathbf{w}, \boldsymbol{\alpha}), \quad J: \mathbb{R}^N \times \mathbb{R}^D \rightarrow \mathbb{R} \tag{2}$$

When searching to minimise a given objective function with respect to the design parameters, the problem usually includes equality and/or inequality constraints, as well as upper and lower bounds imposed on the design parameters in order to limit their variation to some feasible design space. Let all such constraints be given by:

$$\mathbf{G}(\mathbf{w}, \boldsymbol{\alpha}) \leq \mathbf{0}, \quad \mathbf{G}: \mathbb{R}^N \times \mathbb{R}^D \rightarrow \mathbb{R}^K \tag{3}$$

In order to minimize the objective function (2), subject to the equality and inequality constraints given by (3) and to satisfying the system of equations (1) that models the aerodynamic problem, a Lagrange functional can be defined [16]:

$$L(\mathbf{w}, \boldsymbol{\psi}_1, \boldsymbol{\alpha}, \boldsymbol{\psi}_2) = J(\mathbf{w}, \boldsymbol{\alpha}) + (\boldsymbol{\psi}_1, \mathbf{R}(\mathbf{w}, \boldsymbol{\alpha}))_N + (\boldsymbol{\psi}_2, \mathbf{G}(\mathbf{w}, \boldsymbol{\alpha}))_K \tag{4}$$

where $\boldsymbol{\psi}_1 \in \mathbb{R}^N$ and $\boldsymbol{\psi}_2 \in \mathbb{R}^K$ are two sets of Lagrange multipliers, which will also play the role of the adjoint variables.

The critical points of the objective function J will be among the points that cause the Gateaux variation δL of the Lagrange functional (4) to become zero for arbitrary variations of the independent variables, design variables and Lagrange multipliers. The Gateaux variation of (4) is given by:

$$\delta L = \frac{d}{d\varepsilon} [J + \varepsilon \delta J + (\boldsymbol{\psi}_1 + \varepsilon \delta \boldsymbol{\psi}_1, \mathbf{R} + \varepsilon \delta \mathbf{R})_N + (\boldsymbol{\psi}_2 + \varepsilon \delta \boldsymbol{\psi}_2, \mathbf{G} + \varepsilon \delta \mathbf{G})_K] \Big|_{\varepsilon=0} \tag{5}$$

In addition, the following equations can be written:

$$\begin{aligned} \delta J(\mathbf{w}, \boldsymbol{\alpha}) &= \frac{\partial J^T}{\partial \mathbf{w}} \delta \mathbf{w} + \frac{\partial J^T}{\partial \boldsymbol{\alpha}} \delta \boldsymbol{\alpha}, \quad \delta \mathbf{R}(\mathbf{w}, \boldsymbol{\alpha}) = \frac{\partial \mathbf{R}}{\partial \mathbf{w}} \delta \mathbf{w} + \frac{\partial \mathbf{R}}{\partial \boldsymbol{\alpha}} \delta \boldsymbol{\alpha}, \\ \delta \mathbf{G}(\mathbf{w}, \boldsymbol{\alpha}) &= \frac{\partial \mathbf{G}}{\partial \mathbf{w}} \delta \mathbf{w} + \frac{\partial \mathbf{G}}{\partial \boldsymbol{\alpha}} \delta \boldsymbol{\alpha} \end{aligned} \tag{6}$$

All the derivatives appearing in the gradient vectors and Jacobian matrices of (6) are Gateaux partial derivatives.

Introducing (6) into (5), and using the linear properties of the inner product, the Gateaux variation of the Lagrange functional is given by:

$$\begin{aligned} \delta L &= \left(\frac{\partial J}{\partial \mathbf{w}}, \delta \mathbf{w} \right)_N + \left(\frac{\partial J}{\partial \boldsymbol{\alpha}}, \delta \boldsymbol{\alpha} \right)_K + \left(\boldsymbol{\psi}_1, \frac{\partial \mathbf{R}}{\partial \mathbf{w}} \delta \mathbf{w} \right)_N + \left(\boldsymbol{\psi}_1, \frac{\partial \mathbf{R}}{\partial \boldsymbol{\alpha}} \delta \boldsymbol{\alpha} \right)_N + \\ &+ (\mathbf{R}, \delta \boldsymbol{\psi}_1)_N + \left(\boldsymbol{\psi}_2, \frac{\partial \mathbf{G}}{\partial \mathbf{w}} \delta \mathbf{w} \right)_K + \left(\boldsymbol{\psi}_2, \frac{\partial \mathbf{G}}{\partial \boldsymbol{\alpha}} \delta \boldsymbol{\alpha} \right)_K + (\mathbf{G}, \delta \boldsymbol{\psi}_2)_K \end{aligned} \tag{7}$$

In the n -dimensional real space \mathbb{R}^n , a linear operator L^+ is the adjoint to the operator L if the following equation can be written for any two vectors $\mathbf{x}, \mathbf{y} \in \mathbb{R}^n$, where $(,)$ denotes the inner product:

$$(L\mathbf{x}, \mathbf{y}) = (\mathbf{x}, L^+\mathbf{y}) \tag{8}$$

Using the above defined property of adjoint operators, the Jacobian matrices appearing in (7) can be transferred to the Lagrange multipliers and replaced with their corresponding adjoint:

$$\begin{aligned} \delta L = & \left(\frac{\partial J}{\partial \mathbf{w}} + \frac{\partial \mathbf{R}^+}{\partial \mathbf{w}} \boldsymbol{\psi}_1 + \frac{\partial \mathbf{G}^+}{\partial \mathbf{w}} \boldsymbol{\psi}_2, \delta \mathbf{w} \right)_N + (\mathbf{R}, \delta \boldsymbol{\psi}_1)_N + \\ & + \left(\frac{\partial J}{\partial \boldsymbol{\alpha}} + \frac{\partial \mathbf{R}^+}{\partial \boldsymbol{\alpha}} \boldsymbol{\psi}_1 + \frac{\partial \mathbf{G}^+}{\partial \boldsymbol{\alpha}} \boldsymbol{\psi}_2, \delta \boldsymbol{\alpha} \right)_K + (\mathbf{G}, \delta \boldsymbol{\psi}_2)_K \end{aligned} \tag{9}$$

Requiring that the Gateaux variation δL of the Lagrange functional becomes zero for arbitrary variations of the independent variables, design variables and Lagrange multipliers leads to the following set of equations:

$$\frac{\partial J}{\partial \mathbf{w}} + \frac{\partial \mathbf{R}^+}{\partial \mathbf{w}} \boldsymbol{\psi}_1 + \frac{\partial \mathbf{G}^+}{\partial \mathbf{w}} \boldsymbol{\psi}_2 = \mathbf{0} \tag{10}$$

$$\mathbf{R} = \mathbf{0} \tag{11}$$

$$\frac{\partial J}{\partial \boldsymbol{\alpha}} + \frac{\partial \mathbf{R}^+}{\partial \boldsymbol{\alpha}} \boldsymbol{\psi}_1 + \frac{\partial \mathbf{G}^+}{\partial \boldsymbol{\alpha}} \boldsymbol{\psi}_2 = \mathbf{0} \tag{12}$$

$$(\mathbf{G}, \delta \boldsymbol{\psi}_2)_K = 0 \tag{13}$$

The first equation represents the typical adjoint equation found in literature, with an extra term given by the product between the constraints sensitivities to the dependent variables and the second adjoint vector. The second equation is the system of linear or non-linear algebraic equations that defines the aerodynamic model. The third equation contains all the sensitivities with respect to the design variables. The fourth equation is replaced with the equivalent form, following the methodology proposed in [16], [17]:

$$C_i = (G_i + \psi_{2_i})^2 + G_i|G_i| + \psi_{2_i}|\psi_{2_i}|, \quad i = \overline{1, K} \tag{14}$$

Using the equivalence introduced in (14), the set of equations presented in (10) to (13) can be written as a coupled non-linear system:

$$\mathbf{F} = \begin{bmatrix} \frac{\partial J}{\partial \mathbf{w}} + \frac{\partial \mathbf{R}^+}{\partial \mathbf{w}} \boldsymbol{\psi}_1 + \frac{\partial \mathbf{G}^+}{\partial \mathbf{w}} \boldsymbol{\psi}_2 \\ \mathbf{R} \\ \frac{\partial J}{\partial \boldsymbol{\alpha}} + \frac{\partial \mathbf{R}^+}{\partial \boldsymbol{\alpha}} \boldsymbol{\psi}_1 + \frac{\partial \mathbf{G}^+}{\partial \boldsymbol{\alpha}} \boldsymbol{\psi}_2 \\ \mathbf{C} \end{bmatrix} = \mathbf{0}, \quad \mathbf{F}: \mathbb{R}^N \times \mathbb{R}^N \times \mathbb{R}^D \times \mathbb{R}^K \rightarrow \mathbb{R}^{N+N+D+K} \tag{15}$$

The solution of the above system, $(\mathbf{w}, \boldsymbol{\psi}_1, \boldsymbol{\alpha}, \boldsymbol{\psi}_2)^T$, includes the optimal values of the design parameters as required to minimise the objective function J , the solution of the system of equations \mathbf{R} modelling the aerodynamic problem as obtained with the optimal design

parameters, and the values for the two vectors of adjoint variables. In order to obtain the solution of the non-linear system of equations presented in (15), the trust-region method is used [18]. The choice is justified by the fact that numerical tests have shown that the Jacobian matrix of the system may become ill-conditioned or even singular at some points. In the trust-region method, the solution is updated iteratively, starting from an initial guess:

$$\mathbf{x}_{k+1} = \mathbf{x}_k + \Delta \mathbf{x} \quad (16)$$

At each iteration, the solution step is constructed from a convex combination of a Cauchy step, along the steepest descent direction, and a Newton step. The Cauchy step is determined as:

$$\Delta \mathbf{x}_C = -\beta \mathbf{J}(\mathbf{x}_k)^T \mathbf{F}(\mathbf{x}_k) \quad (17)$$

Where the step β is chosen to minimise the trust-region sub-problem, using Powell's efficient dogleg procedure [19]:

$$\min_{\Delta \mathbf{x}_C} \left[\frac{1}{2} \mathbf{F}(\mathbf{x}_k)^T \mathbf{F}(\mathbf{x}_k) + \Delta \mathbf{x}_C^T \mathbf{J}(\mathbf{x}_k)^T \mathbf{F}(\mathbf{x}_k) + \frac{1}{2} \Delta \mathbf{x}_C^T \mathbf{J}(\mathbf{x}_k)^T \mathbf{J}(\mathbf{x}_k) \Delta \mathbf{x}_C \right] \quad (18)$$

The Newton step is calculated by solving the linearized system of equations:

$$\mathbf{J}(\mathbf{x}_k) \Delta \mathbf{x}_N = -\mathbf{F}(\mathbf{x}_k) \quad (19)$$

The step used to update the solution is then computed as a combination between the Cauchy and Newton steps, where λ is a parameter in the interval [0,1]:

$$\Delta \mathbf{x} = \Delta \mathbf{x}_C + \lambda (\Delta \mathbf{x}_N - \Delta \mathbf{x}_C) \quad (20)$$

If the Jacobian matrix is ill-conditioned or singular, then the step is taken only along the Cauchy direction. The trust-region method is computationally efficient, since it requires only one linear system solution per iteration, for the computation of the Newton step, while the Cauchy step requires only matrix-matrix and matrix-vector multiplications, which are computationally inexpensive using vectorised algorithms (such as implemented in the MATLAB software package).

3. CLASSICAL ADJOIT APPROACH

Constructing the adjoint equation in order to eliminate the dependency of the objective function gradient on the flow-field variables, and then using advanced gradient-based optimisation algorithms is today one of the most popular approaches to performing aerodynamic design and optimisation.

The objective function is the one defined in (2), and any variations in the design parameters values cause variations in both the objective function and the system of equations governing the aerodynamic problem:

$$\begin{aligned} \delta J(\mathbf{w}, \boldsymbol{\alpha}) &= \frac{\partial J^T}{\partial \mathbf{w}} \delta \mathbf{w} + \frac{\partial J^T}{\partial \boldsymbol{\alpha}} \delta \boldsymbol{\alpha} \\ \delta \mathbf{R}(\mathbf{w}, \boldsymbol{\alpha}) &= \frac{\partial \mathbf{R}}{\partial \mathbf{w}} \delta \mathbf{w} + \frac{\partial \mathbf{R}}{\partial \boldsymbol{\alpha}} \delta \boldsymbol{\alpha} \end{aligned} \quad (21)$$

It must be kept in mind that the governing equations defined in (1) are solved at each iteration of the optimisation cycle, and thus their variation $\delta \mathbf{R}$ must also be zero. Thus, $\delta \mathbf{R}$

can be multiplied by a Lagrange multiplier and subtracted from the variation δJ without changing the result:

$$\delta J(\mathbf{w}, \boldsymbol{\alpha}) = \left[\frac{\partial J^T}{\partial \mathbf{w}} - \boldsymbol{\psi}^T \frac{\partial \mathbf{R}}{\partial \mathbf{w}} \right] \delta \mathbf{w} + \left[\frac{\partial J^T}{\partial \boldsymbol{\alpha}} - \boldsymbol{\psi}^T \frac{\partial \mathbf{R}}{\partial \boldsymbol{\alpha}} \right] \delta \boldsymbol{\alpha} \quad (22)$$

If the first term of the objective function variation could be set to zero, then the gradient would be independent of the variations of the dependent variables (flow variables) caused by the design parameters variations. Thus, by choosing $\boldsymbol{\psi}$ to satisfy the adjoint equation:

$$\frac{\partial \mathbf{R}^T}{\partial \mathbf{w}} \boldsymbol{\psi} = \frac{\partial J}{\partial \mathbf{w}} \quad (23)$$

The first term is eliminated, and (22) is written as:

$$\delta J(\mathbf{w}, \boldsymbol{\alpha}) = \left[\frac{\partial J^T}{\partial \boldsymbol{\alpha}} - \boldsymbol{\psi}^T \frac{\partial \mathbf{R}}{\partial \boldsymbol{\alpha}} \right] \delta \boldsymbol{\alpha} = \mathbf{G} \delta \boldsymbol{\alpha} \quad (24)$$

The interior point optimisation algorithm also requires the gradient, with respect to the design variables, of any non-linear equality or inequality constraints (such as the one presented in (3)). In order to preserve the computational efficiency of the adjoint method, the constraints that depend on the system dependent variables (flow-field variables) are traditionally not treated as independent functions, but instead are added as a series of penalty terms to the objective function [20]:

$$J(\mathbf{w}, \boldsymbol{\alpha}) \rightarrow J(\mathbf{w}, \boldsymbol{\alpha}) + \lambda_1 G_1(\mathbf{w}, \boldsymbol{\alpha}) + \lambda_2 G_2(\mathbf{w}, \boldsymbol{\alpha}) + \dots \quad (25)$$

This way, the adjoint equation (23) and the gradient defined in (24) must be modified as follows in order to include the constraint:

$$\begin{aligned} \frac{\partial \mathbf{R}^T}{\partial \mathbf{w}} \boldsymbol{\psi} &= \frac{\partial J}{\partial \mathbf{w}} + \lambda_1 \frac{\partial G_1}{\partial \mathbf{w}} + \lambda_2 \frac{\partial G_2}{\partial \mathbf{w}} + \dots \\ \mathbf{G} &= \frac{\partial J^T}{\partial \boldsymbol{\alpha}} + \lambda_1 \frac{\partial G_1}{\partial \boldsymbol{\alpha}} + \lambda_2 \frac{\partial G_2}{\partial \boldsymbol{\alpha}} + \dots - \boldsymbol{\psi}^T \frac{\partial \mathbf{R}}{\partial \boldsymbol{\alpha}} \end{aligned} \quad (26)$$

The interior-point algorithm [21], [22] treats the constrained minimisation problem as a sequence of approximate constrained problems. At each iteration, the method uses one of two possible steps in order to try and minimise the approximate objective function. By default, it tries to solve the Karush-Kuhn-Tucker equations for the approximate problem. If this attempt is unsuccessful, then the algorithm takes a conjugate gradient step. In order to solve the optimisation problem using the interior point method, the algorithm's implementation in the MATLAB software package is used.

4. NON-LINEAR AERODYNAMICS OPTIMISATION PROBLEM

This section of the paper describes the non-linear aerodynamic application, and provides details about the numerical lifting-line model and about the construction of the adjoint-based simultaneous analysis and design system used to solve the proposed optimisation problem.

The numerical method extends the applicability of the lifting-line model to wings having sweep and dihedral, in addition to taper and twisting (geometric and aerodynamic). In this paper, only the important equations of the model are presented, more details being found in

[15] and [23]. The continuous distributions of bound vorticity over the wing surface and of trailing vorticity in the wing wake are approximated using a finite number of N horseshoe vortices. The bound segment of the vortices is aligned with the wing quarter chord line, while the trailing segments are aligned with the direction of the freestream.

The velocity induced by any of the three straight vortex segments making a horseshoe vortex, at an arbitrary point in space, is given by the Biot-Savart law:

$$\mathbf{V} = \frac{\Gamma}{4\pi} \frac{\mathbf{r}_1 \times \mathbf{r}_2}{|\mathbf{r}_1 \times \mathbf{r}_2|^2} \mathbf{r}_0 \left(\frac{\mathbf{r}_1}{r_2} - \frac{\mathbf{r}_2}{r_1} \right) = \frac{\Gamma}{4\pi} \frac{(r_1 + r_2)(\mathbf{r}_1 \times \mathbf{r}_2)}{r_1 r_2 (r_1 r_2 + \mathbf{r}_1 \mathbf{r}_2)} \quad (27)$$

Here, Γ is the vortex intensity, \mathbf{r}_1 and \mathbf{r}_2 are the spatial vectors from the starting and ending points of the straight vortex segment to the arbitrary point in space, r_1 and r_2 are the moduli of the spatial vectors and \mathbf{r}_0 is the spatial vector along the length of the vortex segment. To determine the unknown values of the vortex intensities, the three-dimensional vortex lifting law is applied to express the inviscid force $d\mathbf{F}_i$ acting on the bound segment of each horseshoe vortex:

$$d\mathbf{F}_i = \rho \Gamma_i \mathbf{V}_i \times d\mathbf{l}_i \quad (28)$$

In Eq. (28), $d\mathbf{F}_i$ is the local force acting on a differential segment of the lifting line, a segment that is identical to the bound segment of the horseshoe vortex with an intensity of Γ_i , ρ is the fluid density, \mathbf{V}_i is the local airspeed vector and $d\mathbf{l}_i$ is the spatial vector along the lifting line differential segment, aligned according to the local vorticity. The local airspeed vector over one bound vortex segment is equal to the sum of the freestream velocity \mathbf{V}_∞ and the velocities induced by all the other horseshoe vortices distributed over the wing surface and wake:

$$\mathbf{V}_i = \mathbf{V}_\infty + \sum_{j=1}^N \Gamma_j \mathbf{v}_{ij} \quad (29)$$

where \mathbf{v}_{ij} is the velocity induced at the bound segment of horseshoe vortex i by the unit strength horseshoe vortex j and is given by the sum of three applications of (27) (one for each of the three straight vortex segments making horseshoe vortex j), in which the vortex intensity is considered to be unitary.

From classical wing strip theory, the magnitude of the force acting on a wing strip of area A_i and having a local aerofoil lift coefficient $C_{l_i}^{2D}$ can be written as:

$$\|\mathbf{F}_i\| = \frac{1}{2} \rho V_\infty^2 A_i C_{l_i}^{2D} \quad (30)$$

The local aerofoil lift coefficient can be determined using other means, such as experimentally determined lift curves or 2D simulations using fast, coupled panel methods/boundary layer codes, provided that the local strip angle of attack is known. This local effective angle of attack α_{eff_i} can be calculated using the local strip velocity \mathbf{V}_i , the local aerofoil chord-wise unit vector \mathbf{c}_i and the unit vector normal to the local aerofoil chord \mathbf{n}_i , and is given by:

$$\alpha_{eff_i} = \tan^{-1} \left(\frac{\mathbf{V}_i \mathbf{n}_i}{\mathbf{V}_i \mathbf{c}_i} \right) \quad (31)$$

If the wing strips are taken such that each horseshoe vortex-bound segment corresponds to one strip, then the modulus of the force given by Eq. (30) can be set equal to the one given

by Eq. (28), since the bound segment is the only segment upon which the surrounding fluid exerts a force, the trailing segments being aligned with the freestream. Thus, for the vortex system over the wing surface, the following non-linear system can be written:

$$\left\| \rho \Gamma_i \left(\mathbf{v}_\infty + \sum_{j=1}^N \Gamma_j \mathbf{v}_{ij} \right) \times \mathbf{dl}_i \right\| - \frac{1}{2} \rho V_\infty^2 A_i C_i^{2D} = 0, \quad i = 1, 2, \dots, N \quad (32)$$

Once all of the horseshoe vortices' intensities have been calculated by solving the non-linear system presented above, the aerodynamic force and moment about the root chord quarter chord point can be immediately determined:

$$\mathbf{F} = \rho \sum_{i=1}^N \left[\left(\mathbf{v}_\infty + \sum_{j=1}^N \Gamma_j \mathbf{v}_{ij} \right) \Gamma_i \times \mathbf{dl}_i \right] \quad (33)$$

$$\mathbf{M} = \rho \sum_{i=1}^N \mathbf{r}_i \times \left[\left(\mathbf{v}_\infty + \sum_{j=1}^N \Gamma_j \mathbf{v}_{ij} \right) \Gamma_i \times \mathbf{dl}_i \right] + \frac{1}{2} \rho V_\infty^2 A_i c_i C_{m_i}^{2D} (\mathbf{c}_i \times \mathbf{n}_i) \quad (34)$$

In recent years, the development and application of morphing solutions on Unmanned Aerial Vehicles (UAVs) has garnered considerable interest, due to the increasingly greater efficiency requirements and their much simpler certification issues, compared to manned airplanes. Various researchers have presented concepts for morphing UAVs that achieved performance improvements over the traditional, fixed geometry versions. Barbarino et al. [24] performed an extensive review of aircraft morphing technologies and their applications. The main advantage of actively modifying the wing shape using a morphing technique is that an optimal shape for the wing and/or aerofoil can be provided during each distinct phase of the UAV flight, for each of the various airflow conditions. One promising solution that could efficiently increase a wing's lift-to-drag ratio is the morphing wing-tip [25], [26]. This morphing device could be retrofitted on existing wings with only a relatively small and localised increase of the design complexity, due to the addition of the servo-actuated mechanisms at the wing's tip [25]. For the purpose of the present study, a baseline wing with winglet geometry is selected, with the winglet considered to have a morphing toe angle. The aerodynamic model is provided by the numerical non-linear lifting-line method.

The following optimisation problem is formulated: for a given baseline wing plan-form and winglet shape and for a given range of flight conditions, determine the optimal winglet toe angles that achieve higher single-point lift-to-drag ratios, compared to the baseline geometry. The optimisation problem attempted can be summarised as follows:

for each selected flight condition:

$$\text{maximize: } J = \frac{L}{D}$$

with respect to: winglet toe angle

$$\text{subject to: } -10^\circ \leq \text{winglet toe angle} \leq 10^\circ \quad (35)$$

It must be pointed out that the objective of this application is to quantify the performance of the adjoint-based simultaneous analysis and design approach compared to the adjoint gradient-based optimisation technique, using non-linear numerical aerodynamic

models. It is not intended to design an efficient morphing-wing concept, and thus the baseline geometry is chosen without performing a multi-point design process, while the selected flight conditions are not based on investigating flight performance metrics for a specific UAV model. The dependent variables for the non-linear problem are the horseshoe vortex intensities, $\mathbf{w} = \boldsymbol{\Gamma}$, while the design parameters are represented by the two morphing winglet toe angles, $\boldsymbol{\alpha} = (\tau_1, \tau_2)$. The space of the dependent parameters \mathbb{R}^N has a dimension equal to the chosen number of span-wise horseshoe vortices N , while the space of the design parameters \mathbb{R}^D has a dimension of $D = 2$. The system of equations describing the aerodynamic model is represented by the equations presented in (32), and thus:

$$R_i(\mathbf{w}, \boldsymbol{\alpha}) = \left\| \rho \Gamma_i \left(\mathbf{V}_\infty + \sum_{j=1}^N \Gamma_j \mathbf{v}_{ij} \right) \times \mathbf{d}\mathbf{l}_i \right\| - \frac{1}{2} \rho V_\infty^2 A_i C_{l\alpha_i}^{2D} \left(\tan^{-1} \left[\frac{(\mathbf{V}_\infty + \sum_{j=1}^N \Gamma_j \mathbf{v}_{ij}) \mathbf{n}_i}{(\mathbf{V}_\infty + \sum_{j=1}^N \Gamma_j \mathbf{v}_{ij}) \mathbf{c}_i} \right] - \alpha_{0i} \right) = 0, \quad i = 1, 2, \dots, N \tag{36}$$

The dependence of the equations presented above on the design parameters is achieved through the local chord-wise unit vectors \mathbf{c}_i and the local normal unit vectors \mathbf{n}_i for the winglets, which change as the two toe angles vary. Furthermore, it is assumed that the morphing of the winglets as a function of the toe angles is done as a rotation around their quarter-chord lines. Thus, the spatial vectors $\mathbf{d}\mathbf{l}_i$ along the lifting line segments and the induced velocities \mathbf{v}_{ij} remain independent of the toe angles values.

The bounds and constraints are given by the following equation, and thus the space of the constraints \mathbb{R}^K has a dimension of $K = 4$:

$$\mathbf{G}(\mathbf{w}, \boldsymbol{\alpha}) = \begin{Bmatrix} \tau_{min} - \tau_1 \\ \tau_1 - \tau_{max} \\ \tau_{min} - \tau_2 \\ \tau_2 - \tau_{max} \end{Bmatrix} \leq \mathbf{0} \tag{37}$$

All terms appearing in the non-linear system (15), and in the Jacobian matrix required for the Newton step (19) of the trust-region method were analytically determined, but are not presented in the paper due to the length of the obtained equations.

5. RESULTS AND DISCUSSIONS

The geometrical characteristics of the chosen wing with winglets are presented in Table 1. As mentioned earlier in the paper, the focus is not on designing an efficient morphing-wing concept, and thus the baseline geometry is chosen without performing a multi-point design process, while the selected flight conditions are not based on investigating flight performance metrics for a specific UAV model.

Table 1 – Wing and Winglets Geometry Parameters

Parameter	Value
Wing Root Chord [m]	0.10
Wing Taper Ratio	0.70
Span-Wise Chord Variation	Linear
Wing Span [m]	1
Wing Aspect Ratio	11.75

Wing Sweep [°]	0
Wing Geometric Twist [°]	No Twist
Wing Aerofoil Section	NACA 4412
Winglet Root Chord [m]	0.07
Winglet Taper Ratio	0.70
Winglet Span [m]	0.10
Winglet Sweep [°]	0
Winglet Cant Angle [°]	0
Winglet Initial Toe Angle [°]	0
Winglet Aerofoil Section	NACA 4409

The optimisations are performed at an airspeed of 10 m/s, for three angle of attack values: -3° , 0° and 3° . The wing is modelled using 60 horseshoe vortices, clustered towards the wing tips, while 20 horseshoe vortices are used for each winglet, clustered towards both the winglet tip and the junction with the wing tip. The lift curve slope and the zero-lift angle of attack for both wing and winglet aerofoils are taken from experimental data. The drag computations are limited to the induced drag component. For all optimisation runs, toe angles values are bounded between a lower limit of $\tau_{min} = -10^\circ$ and an upper limit of $\tau_{max} = 10^\circ$. The trust-region algorithm used for solving the nonlinear system of the adjoint simultaneous analysis and design approach is configured to stop when both the norm of the linearized system residual $\|F(x_k)\|$ and the norm of the solution change between two consecutive steps $\|\Delta x\|$ become smaller than 10^{-10} .

For the interior-point optimisation with adjoint-based gradient calculation, an objective function tolerance, a solution tolerance of and a constraints tolerance equal to 10^{-10} are used. All considered convergence criteria must be satisfied in order to accept the optimisation results. In addition, the convergence criteria for the iterative solution of the nonlinear lifting line system of equations is set to 10^{-10} , using the trust-region algorithm.

It must be noted that both optimisation approaches converge towards the same solution in terms of the design parameters (the two toe angles values), to an order of accuracy of two significant digits. Table 2 presents a comparison between the lift-to-drag ratio for the original design and for the optimised design, together with the toe angles values the morphing winglets take at each different angle of attack in order to achieve the indicated performance increase.

Table 2 – Performance Improvements Obtained Using Morphing Winglet

Parameter	Original $\frac{C_L}{C_D}$	Optimized $\frac{C_L}{C_D}$	Winglet 1 Toe [°]	Winglet 2 Toe [°]
Angle of attack [°]				
-3	19.07	21.10	-6.3208	6.3208
0	45.49	48.94	-5.9850	5.9850
3	42.31	44.55	-6.1178	6.1178

Figure 1 presents the span-wise loading, defined in terms of both lift coefficient and induced drag coefficient, for the original and optimised geometries at the three chosen angle of attack values. The loading is calculated as the ratio of the sectional coefficient to the wing coefficient multiplied with the ratio of the sectional chord to the mean aerodynamic chord. The results are shown only for the wing surface itself, not for the winglets. It can be seen that changing the winglet toe angles influences the circulation distribution over the entire span, the effect being the strongest towards the wing tip. An increase in the lift distribution is obtained, with a corresponding increase in induced drag. Overall, the lift-to-drag increases, as the obtained benefits outweigh the drag increase. Figure 2 shows the convergence of the

non-linear system residual $\|F(x_k)\|$ or of the objective function J together with the number of system solutions required, as function of the iteration number, for the 3° angle of attack optimisation case. The vertical axis of both plots uses a logarithmic scaling.

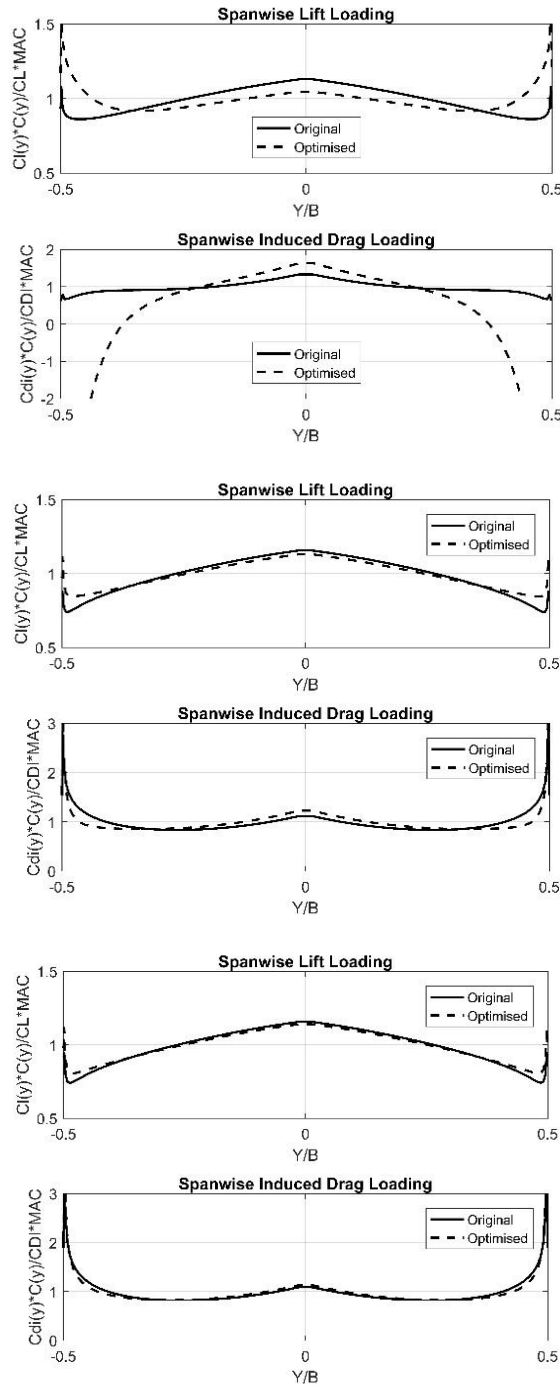


Fig. 1 – Comparison between the lift and induced drag span-wise loading between the original and optimized wing geometries, at angles of attack of -3 deg. (top two plots), 0 deg. (middle two plots) and 3 deg. (bottom two plots)

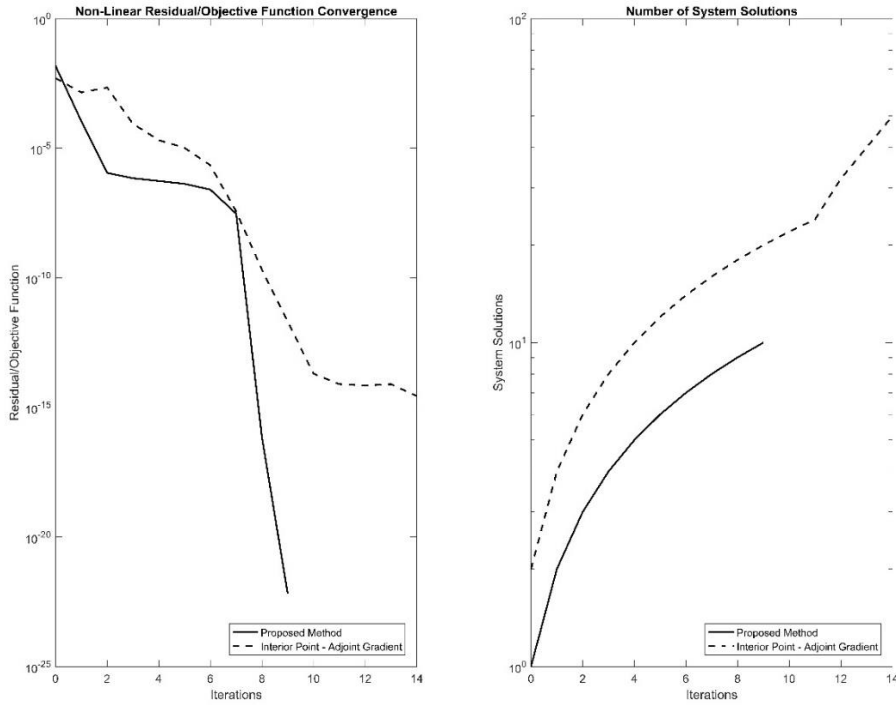


Fig. 2 – Convergence and computational effort of the two adjoint-based optimization approaches for the 3° angle of attack optimization case

Before discussing the relative performance of the algorithms, it must be kept in mind that the linearized system obtained for the Newton step of the trust-region method is a system of $(N + N + D + K)$ equations, while for the interior point optimisation method, the aerodynamic model equations or the adjoint equations are only of size N .

Considering that the solution process of a linear system of equations requires $O(N^3)$ operations (achievable when using the high-performance linear solvers implemented in MATLAB), the computational effort per linear system solution is higher with the proposed method.

Table 3 summarises the number of iterations requires to achieve convergence and the total number of system solutions (either linear or non-linear) performed during the optimisation process, for both optimisation approaches and for all three optimisation cases.

In the case of the adjoint simultaneous method, one iteration means one linear system solution (the Newton step of equation (19)), but in the case of the interior point method, one iteration means one solution of the non-linear aerodynamics system (given by (36)) and one linear system solution (the adjoint equations (26)).

In addition, the number of system solutions (both non-linear and linear) per iteration is sometimes higher than two because of the two-step approach used by the interior point optimisation algorithm.

However, the total number of solutions will always be an even number, half of those being solving the non-linear aerodynamics system.

Table 3 – Comparison of Algorithm Performance

Algorithm	Adjoint Simultaneous Analysis and Design		Interior Point with Adjoint Gradient	
	Iterations	System Solutions (Linear)	Iterations	System Solutions (Linear + Non-linear)
Angle of attack [°]				
-3	7	7	16	48
0	15	15	18	66
3	10	10	14	50

As was mentioned, the non-linear lifting line system of equations is also solved using the trust-region algorithm.

However, because the Jacobian matrix is always non-singular and well-conditioned, the algorithm reduces to the simple Newton method.

A closer inspection of the solution process reveals that 10 iterations (comprising 10 linear system solutions) are sufficient to achieve the desired convergence criteria of 10^{-10} . Table 4 presents another comparison between the two optimisation approaches, but only in terms of total number of linear system solutions.

Table 4 – Comparison of Algorithm Performance (Only Linear System Solutions)

Algorithm	Adjoint Simultaneous Analysis and Design		Interior Point with Adjoint Gradient	
	Iterations	System Solutions	Iterations	System Solutions
Angle of attack [°]				
-3	7	7	16	264
0	15	15	18	366
3	10	10	14	275

It can be observed that the number of iterations required by the adjoint simultaneous method is slightly lower than the interior-point optimisation method.

The linear system obtained by applying the simultaneous method for this problem is a system of $(N + N + 2 + 4) = (2N + 6)$ equations, with $N = 100$.

Thus, one solution of the $(2N + 6)$ linear system requires approximately $O((2N + 6)^3) \approx 8 \cdot O(N^3)$, thus 8 times more operations than one solution a N size linear system.

Looking over the results presented in Table 4, it is immediately seen that even with the significantly higher computational effort per linear system solution (due to the larger matrices), the overall number of operations required by the simultaneous method is much smaller compared to the gradient-based optimization algorithm using adjoint-determined gradient.

Thus, the adjoint-based simultaneous approach is more computationally efficient than the gradient-based optimisation approach for non-linear aerodynamic problems of interest having a high number of dependent variables and a relatively low number of design parameters.

This is the case for many problems of engineering interest, not only conceptual aerodynamic design using potential-flow methods.

6. CONCLUSIONS

In this paper, an adjoint-based simultaneous analysis and design method was presented and applied for a non-linear constrained aerodynamic optimisation problem. It was formulated using a numerical non-linear lifting line method and aimed at determining the optimal winglet toe angle for a wing concept equipped with morphing winglets.

The number of design parameters was much smaller compared to the number of dependent variables, as is the case for most problems of practical interest. Comparisons against the interior point algorithm using the traditional adjoint gradient calculation showed that the simultaneous approach was much more efficient in terms of the computational effort required, defined in terms of the total number of linear system solutions.

REFERENCES

- [1] G. Carrier, D. Destarac, A. Dumont, M. Meheut, I. S. E. Din, J. Peter, S. B. Khelil, J. Brezillon and M. Pestana, *Gradient-Based Aerodynamic Optimization With the elsA Software*, 52nd AIAA Aerospace Sciences Meeting. AIAA Paper 2014-0568, 2014.
- [2] A. Jameson, Aerodynamic Design via Control Theory. *Journal of Scientific Computing*, Vol. **3**, No. 3, pp. 233-260, 1988.
- [3] A. Jameson, Optimum Aerodynamic Design Using CFD and Control Theory, *AIAA Paper 1995-1729*, 1995.
- [4] K. Sermeus, K. Mohamed, E. Laurendeau and S. Nadarajah, *Development of an Industrial Aerodynamic Shape Optimization Strategy Using a Discrete Adjoint Method*, 18th Annual Conference of the CFD Society of Canada, London, ON, Canada, 2010.
- [5] S. Nadarajah and A. Jameson, A comparison of the continuous and discrete adjoint approach to automatic aerodynamic optimization, *AIAA Paper 2000-0667*, 2000.
- [6] E. Fabiano, A. Mishra, D. Mavriplis and K. Mani, *Time-Dependent Aero-acoustic Adjoint-based Shape Optimization of Helicopter Rotors in Forward Flight*, 57th AIAA/ASCE/AHS/ASC Structures, Structural Dynamics, and Materials Conference, *AIAA Paper 2016-1910*, 2016.
- [7] T. Blacha, M. M. Gregersen, M. Islam and H. Bensler, *Application of the Adjoint Method for Vehicle Aerodynamic Optimization*, SAE 2016 World Congress and Exhibition, *SAE Technical Paper 2016-01-1615*, 2016.
- [8] G. K. W. Kenway and J. R. R. A. Martins, Multipoint High-Fidelity Aerostructural Optimization of a Transport Aircraft Configuration, *Journal of Aircraft*, Vol. **51**, No. 1, pp. 144-160, 2014.
- [9] J. Reuther, J. J. Alonso, M. J. Rimlinger and A. Jameson, Aerodynamic Shape Optimization of Supersonic Aircraft Configurations via an Adjoint Formulation on Distributed Memory Parallel Computers, *Computers & fluids*, Vol. **28**, No. 4, pp. 675-700, 1999.
- [10] S. W. Funke, P. E. Farrell and M. D. Piggott, Tidal Turbine Array Optimisation Using the Adjoint Approach. *Renewable Energy*, Vol. **63**, pp. 658-673, 2014.
- [11] S. A. Ragab, Shape Optimization of Surface Ships in Potential Flow Using an Adjoint Formulation, *AIAA Journal*, Vol. **42**, No. 2, pp. 296-304, 2004.
- [12] O. Polat and I. H. Tuncer, Aerodynamic Shape Optimization of Wind Turbine Blades Using a Parallel Genetic Algorithm. *Procedia Engineering*, Vol. **61**, pp. 28-31, 2013.
- [13] O. Şugar Gabor, A. Koreanschi, R. M. Botez, M. Mamou and Y. Mebarki, Numerical simulation and wind tunnel tests investigation and validation of a morphing wing-tip demonstrator aerodynamic performance, *Aerospace Science and Technology*, Vol. **53**, pp. 136-153, 2016.
- [14] A. Koreanschi, O. Sugar-Gabor and R. M. Botez, Drag Optimisation of a Wing Equipped With a Morphing Upper Surface, *The Aeronautical Journal*, Vol. **120**, No. 1225, pp. 473-493, 2016.
- [15] O. Şugar Gabor, A. Koreanschi and R. M. Botez, Analysis of UAS-S4 Éhecatl Aerodynamic Performance Improvement Using Several Configurations of a Morphing Wing Technology, *The Aeronautical Journal*, Vol. **120**, No. 1231, pp. 1337-1364, 2016.
- [16] D. G. Cacuci, *Sensitivity and Uncertainty Analysis, Volume I: Theory*, Boca Raton, FL, USA: CRC Press, ISBN 9781584881155, 2003.
- [17] D. G. Cacuci, M. Ionescu-Bujor and I. M. Navon, *Sensitivity and Uncertainty Analysis, Volume II: Applications to Large-Scale Systems*, Boca Raton, FL, USA: CRC Press, 2005.
- [18] R. H. Byrd, J. C. Gilbert and J. A. Nocedal, Trust Region Method Based on Interior Point Techniques for Nonlinear Programming, *Mathematical Programming*, Vol. **89**, No. 1, pp. 149-185, 2000.
- [19] M. J. D. Powell, *A FORTRAN Subroutine for Solving Systems of Nonlinear Algebraic Equations*, Atomic Energy Research Establishment, Harwell (England), 1968.
- [20] M. B. Giles and N. A. Pierce, An Introduction to the Adjoint Approach to Design, *Flow, Turbulence and Combustion*, Vol. **65**, No. 3-4, pp. 393-415, 2000.
- [21] J. Nocedal and S. V. Wright, *Numerical Optimization*, New York, NY, USA: Springer Science & Business Media, Second Edition, ISBN-10: 0-387-30303-0, ISBN-13: 978-0387-30303-1, 2006.

- [22] R. A. Waltz, J. L. Morales, J. Nocedal and D. Orban, An Interior Algorithm for Nonlinear Optimization that Combines Line Search and Trust Region Steps, *Mathematical Programming*, Vol. **107**, No. 3, pp. 391-408, 2006.
- [23] W. F. Phillips and D. O. Snyder, Modern adaptation of Prandtl's classic lifting-line theory, *Journal of Aircraft*, Vol. **37**, Issue 4, pp. 662-670, 2000.
- [24] S. Barbarino, O. Bilgen, R. M. Ajaj, M. I. Friswell and D. J. Inman, A Review of Morphing Aircraft, *Journal of Intelligent Material Systems and Structures*, Vol. **22**, Issue 9, pp. 823-877, 2011.
- [25] L. Falcão, A. A. Gomes and A. Suleman, Aero-Structural Design Optimization of a Morphing Wingtip, *Journal of Intelligent Material Systems and Structures*, Vol. **22**, Issue 10, pp.1113-1124, 2011.
- [26] D. D. Smith, R. M. Ajaj, A. T. Isikveren and M. I. Friswell, Multi-Objective Optimization for the Multiphase Design of Active Polymorphing Wings, *Journal of Aircraft*, Vol. **49**, Issue 4, pp.1153-1160, 2012.